doi:10.1093/brain/awab093 BRAIN 2021: 144; 1697–1710 | 1697

BRAIN
ORIGINAL ARTICLE

Formation and immunomodulatory function of meningeal B cell aggregates in progressive CNS autoimmunity

Meike Mitsdoerffer,[1,2] Giovanni Di Liberto,[3] Sarah Dötsch,[4] Christopher Sie,[2] Ingrid Wagner,[3] Monika Pfaller,[2] Mario Kreutzfeldt,[3] Simon Fräßle,[4] Lilian Aly,[1] Benjamin Knier,[1] Dirk H. Busch,[4,5] Doron Merkler[3] and Thomas Korn[1,2,6]

Meningeal B lymphocyte aggregates have been described in autopsy material of patients with chronic multiple sclerosis. The presence of meningeal B cell aggregates has been correlated with worse disease. However, the functional role of these meningeal B cell aggregates is not understood.

Here, we use a mouse model of multiple sclerosis, the spontaneous opticospinal encephalomyelitis model, which is built on the double transgenic expression of myelin oligodendrocyte glycoprotein-specific T-cell and B-cell receptors, to show that the formation of meningeal B cell aggregates is dependent on the expression of α4 integrins by antigen-specific T cells. T cell-conditional genetic ablation of α4 integrins in opticospinal encephalomyelitis mice impaired the formation of meningeal B cell aggregates, and surprisingly, led to a higher disease incidence as compared to opticospinal encephalomyelitis mice with α4 integrin-sufficient T cells. B cell-conditional ablation of α4 integrins in opticospinal encephalomyelitis mice resulted in the entire abrogation of the formation of meningeal B cell aggregates, and opticospinal encephalomyelitis mice with α4 integrin-deficient B cells suffered from a higher disease burden than regular opticospinal encephalomyelitis mice. While anti-CD20 antibody-mediated systemic depletion of B cells in opticospinal encephalomyelitis mice after onset of disease failed to efficiently decrease meningeal B cell aggregates without significantly modulating disease progression, treatment with anti-CD19 chimeric antigen receptor-T cells eliminated meningeal B cell aggregates and exacerbated clinical disease in opticospinal encephalomyelitis mice. Since about 20% of B cells in organized meningeal B cell aggregates produced either IL-10 or IL-35, we propose that meningeal B cell aggregates might also have an immunoregulatory function as to the immunopathology in adjacent spinal cord white matter. The immunoregulatory function of meningeal B cell aggregates needs to be considered when designing highly efficient therapies directed against meningeal B cell aggregates for clinical application in multiple sclerosis.

1 Klinikum rechts der Isar, Department of Neurology, Technical University of Munich, 81675 Munich, Germany
2 Klinikum rechts der Isar, Institute for Experimental Neuroimmunology, Technical University of Munich, 81675 Munich, Germany
3 Division of Clinical Pathology, Department of Pathology and Immunology, Geneva Faculty of Medicine, Centre Médical Universitaire, 1211 Geneva, Switzerland
4 Institute for Medical Microbiology, Immunology, and Hygiene, Technical University of Munich, 81675 Munich, Germany
5 National Center for Infection Research (DZIF), Technical University of Munich, 81675 Munich, Germany
6 Munich Cluster for Systems Neurology (SyNergy), DZNE site Munich, 81377 Munich, Germany

Received October 22, 2020. Revised January 18, 2021. Accepted January 19, 2021. Advance access publication March 9, 2021

Correspondence to: Thomas Korn
Klinikum rechts der Isar, Technical University of Munich
Institute for Experimental Neuroimmunology
Ismaninger Str. 22, 81675 Munich, Germany
E-mail: thomas.korn@tum.de

Keywords: B cell; meningeal inflammation; multiple sclerosis; experimental autoimmune encephalomyelitis; CAR T cell

Abbreviations: CAR = chimeric antigen receptor; EAE = experimental autoimmune encephalomyelitis; MEBAG = meningeal B cell aggregate; OSE = opticospinal encephalomyelitis

Introduction

B lymphocyte aggregates have been identified in the meningeal space of patients with secondary progressive multiple sclerosis.[1] CD35$^+$ follicular dendritic cells[1] and proliferating (Ki67$^+$) B cells[2] were identified in these B cell aggregates. Therefore, they have been considered as tertiary lymphoid tissue with bona fide B cell follicles.[1,2] B cell follicles are highly organized structures where class switch recombination and somatic hypermutation is induced in specific B cell clones by repeated rounds of cognate interaction with T follicular helper cells.[3] Eventually, germinal centre (GC) B cells develop into plasma blasts that produce affinity matured antibodies. It is possible that meningeal B cell aggregates (MEBAGs) contribute to immunopathology in multiple sclerosis. For instance, by secretion of autoantibodies, demyelination in adjacent cortical areas could be promoted, which was inferred by the finding that demyelinated areas of the cortex were identified in close proximity with MEBAGs.[2] However, while the compilation of these observations is intriguing, only few mechanistic studies have addressed the function of MEBAGs for the promotion of immunopathology in CNS autoimmunity.

In fact, it is possible that MEBAGs develop in the meningeal compartment in a counterregulatory process in response to ongoing inflammation. Intriguingly, the combined neutralization of the B cell growth and maturation factors BAFF and APRIL[4] exacerbated multiple sclerosis in a dose dependent manner.[5] Moreover, B cells were shown to contribute to dampening inflammatory responses by secretion of regulatory cytokines including IL-10[6] and IL-35,[7] and IgA producing plasma cells mitigated the severity of experimental autoimmune encephalomyelitis (EAE) by acting within the CNS compartment.[8]

Th17 cells were shown to contribute to the creation of a stromal niche in the meninges to support the development of MEBAGs, and the lymphotoxin (LT)βR ligands expressed by Th17 cells appear to license meningeal stromal cells for this task in SJL/J mice.[9] Also, IL-17 and podoplanin produced by Th17 cells were suggested to induce MEBAGs during EAE.[10] Notably, during the development of secondary lymphoid tissue in ontogenesis, lymphoid tissue inducer cells rely on the expression of α4 integrins for entering the stromal niche that later accommodates secondary lymphoid tissue.[11]

The analysis of MEBAGs has been hampered because MOG(35–55)-induced EAE, the most widely used animal model for multiple sclerosis, essentially lacks B cell aggregates in the meninges.[12] Immunization of mice with recombinant MOG protein instead of MOG(35–55) peptide engages B cells as antigen presenting cells (APCs), and has been used to show that MHC class II expression and interaction with T cells rather than secretion of antibodies is essential for the generation of immunopathology in EAE.[13] However, the abundance of MEBAGs is very low even in EAE induced with recombinant MOG protein.[12] In contrast, in the spontaneous model of EAE, the opticospinal encephalomyelitis (OSE) mouse, in which both T cells[14] and B cells[15] express a MOG-specific antigen receptor, MEBAGs develop in abundance.[16,17]

In this study, we exploited the OSE mouse model to investigate the role of α4 integrins in T cells and B cells for the generation of MEBAGs in the subarachnoid space. Conditional genetic ablation of *Itga4*, which encodes α4 integrins, in T cells led to the reduced formation of MEBAGs in OSE mice. Yet, the incidence of spontaneous EAE was increased in these mice as compared to regular OSE mice. B cell-conditional *Itga4*$^{-/-}$ OSE mice lacked MEBAGs and developed a higher disease burden than their wild-type OSE littermates. While B cell depletion in presymptomatic OSE mice using a monoclonal anti-CD20 antibody alleviated disease development, the same treatment did not significantly modulate disease progression when started in symptomatic OSE mice with already established MEBAGs. Anti-CD20 antibodies only partially reduced MEBAGs. In contrast, anti-CD19 chimeric antigen receptor (CAR)-T cell application essentially eliminated MEBAGs, and significantly enhanced a chronic progressive disease course in OSE mice. Together, these data indicated that MEBAGs might support immunoregulatory processes in compartmentalized CNS inflammation, challenging the view that efficient meningeal B cell depletion might be a uniformly beneficial therapeutic intervention to halt chronic progression in multiple sclerosis.

Materials and methods

Mice

TCR^{MOG} (2D2) mice,[14] BCR$^{MOG,\ KI/KI}$ (TH) mice,[15] *Itga4*$^{flox/flox}$ mice,[18] *Cd4-Cre* mice,[19] and *Cd19-Cre* mice[20] have been previously reported. The OSE mouse has also been described previously.[16,17] In addition to regular OSE mice (2D2; TH), we bred T cell-conditional α4 integrin deficient OSE mice (2D2; TH; *Itga4*$^{flox/flox}$; *Cd4-Cre*) as well as B cell-conditional α4 integrin deficient OSE mice (2D2; TH; *Itga4*$^{flox/flox}$; *Cd19-Cre*$^{wt/KI}$) for this study and termed them OSE-*Itga4*$^{\Delta T}$ and OSE-*Itga4*$^{\Delta B}$ mice, respectively. All mice were on pure C57BL/6 background and were kept in the facilities of the Technical University of Munich according to the local guidelines for animal welfare and experimentation (TVA AZ: ROB-55.2-2532.Vet_02-13-29, ROB-55.2-2532.Vet_02-17-69, ROB-55.2-2532.Vet_02-17-234, ROB-55.2-2532.Vet_02-14-95, ROB-55.2-2532.Vet_03-18-53).

Retroviral vector construction

The previously described second-generation murine m1928E CAR construct[21] was used for retroviral transduction of primary murine splenocytes. The construct contains a murine anti-murine CD19

single chain variable fragment (scFv) fused—via a CD8-derived extracellular and transmembrane domain—to the intracellular CD28 costimulatory domain and the CD3 ζ signalling domain, which were synthesized into a retroviral pMP71 vector (kindly provided by Wolfgang Uckert, MDB Berlin, Germany). For selection via cell sorting, this gene construct is connected—via a P2A linker—to a truncated, functionally inert version of the epidermal growth factor receptor (EGFRt[22]; kindly provided by Stanley Riddell, Fred Hutchinson Cancer Research Center, USA).

Cell culture and retroviral transduction

Murine T cells were cultivated in RPMI 1640 (Gibco), supplemented with 10% foetal calf serum (FCS), 0.025% L-glutamine, 0.1% HEPES, 0.001% gentamycin, 0.002% streptomycin, and 25 U/ml IL-2. Platinum-E cells were grown in Dulbecco's modified Eagle medium (DMEM) (Gibco), supplemented with 10% FCS, 0.025% L-glutamine, 0.1% HEPES, 0.001% gentamycin, and 0.002% streptomycin.

The CAR construct was retrovirally transduced into murine splenocytes obtained from wild-type C57BL/6 mouse spleens using Platinum-E cells. Primary mouse splenocytes were brought into single-cell suspension, incubated in erythrocyte lysis buffer once and stimulated overnight with purified anti-mouse CD3 (1:1000, clone 145-2C11, BD Pharmingen) and anti-mouse CD28 (1:3000, clone 37.51, BD Pharmingen) antibodies, as well as 25 U/ml IL-2. For retroviral particle production, RD114 cells were transfected with pMP71 expression vector (containing the CAR construct, gag/pol and amphotropic envelope) by calcium phosphate precipitation. Virus supernatant was filtered through 0.45-μm pore filters and spin-oculated onto plates coated with RetroNectin® (Takara Bio Europe SAS) at 3000*g* at 32°C for 2 h. Stimulated mouse splenocytes were added to the plates and centrifuged at 800*g* at 32°C for 90 min. Transduced splenocytes were expanded for 2 days. Transduced $EGFR^+$ $CD19^-$ splenocytes were then sorted by flow cytometry (CAR-T cells) and used for adoptive transfer. To produce control cells, C57BL/6 splenocytes were similarly activated but left untransduced. These splenocytes were then also sorted for $CD19^-$ cells and used as control cells in the adoptive transfer experiments.

Antibody staining and flow cytometry sorting

After retroviral transduction and expansion, transduced T cells were sorted using a MoFloII Cell Sorter (Beckman Coulter) or FACSAria (BD Biosciences) on $EGFRt^+$ cells after staining with anti-EGFR antibody (BioLegend). Cells were stained with the respective antibody panel in the dark at 4°C for 20 min. Staining with anti-mouse CD19 monoclonal antibody (clone 1D3, PECF594, BD Pharmingen) and propidium iodide (Invitrogen) was added to allow for exclusion of B cells and dead cells.

Spontaneous EAE and *in vivo* treatments

Spontaneous EAE in regular OSE mice, OSE-$Itga4^{\Delta T}$ and OSE-$Itga4^{\Delta B}$ mice was monitored daily as described previously.[23] To deplete B cells, mice received the anti-CD20 antibody 18B12 intraperitoneally once a week (10 μg/g weight) or the respective control antibody MOPC-21 (IgG1). Treatment was either initiated before onset of disease at the age of 4 weeks or after onset of disease as soon as mice reached a score of ⩾2. Alternatively, we used CD19-directed CAR-T cells for depletion of B cells. In this case mice were irradiated with 2.5 Gy at the age of 4–5 weeks. One day later, they received 1–2 × 10^6 CAR-T cells or control cells intravenously.

Adoptive transfer experiment

Naïve ($CD4^+CD44^-CD25^-$) 2D2 T cells were isolated by flow cytometric sorting from lymph nodes and spleens of α4 integrin deficient 2D2 mice (2D2; $Itga4^{flox/flox}$; *Cd4-Cre*) or corresponding 2D2 control mice. T cells were then loaded with proliferation dye eFluor® 450 (Invitrogen) according to the manufacturer's instructions and 3 × 10^6 cells per mouse were transferred intravenously into BCR^{MOG} mice on Day –1. On Days 0 and 1, mice were immunized intravenously with 20 μg MOG(35–55) peptide in PBS. Control mice received only PBS. On Day 4, cells were isolated from the spleen of recipient mice, stimulated with PMA (50 ng/ml) and ionomycin (1 μg/ml) for 2.5 h at 37°C in the presence of monensin (1 μl/ml BD GolgiStop), stained for live/dead fixable dye, surface markers (CD4, Vα3.2, Vβ11), and intracellular cytokines (IFN-γ, IL-17) as described,[24] and analysed on a CytoFLEX flow cytometer (Beckman Coulter). Flow cytometric data were analysed with FlowJo (BD, Version 10.7.1).

Histology including determination of MEBAG area and Mac-3 signal quantification

Mice were perfused with cold PBS followed by 4% paraformaldehyde fixation (pH 7.4). Brain and spinal cord were dissected and embedded in paraffin. Antigen retrieval was performed on 3-μm thick sections according to standardized protocols by heating with citrate buffer (pH 6). Endogenous peroxidases were neutralized (peroxidase blocking reagent, Dako), and non-specific binding of antibodies was blocked for 5 min with PBS/1% BSA/2% FCS. For immunohistochemistry, sections were incubated with rat anti-mouse B220 (clone RA3-6B2, eBioscience), polyclonal rabbit anti-mouse CD3 (Dako) or rat anti-mouse Mac-3 (clone M3/84). Horseradish peroxidase (HRP)-coupled goat anti-rat or goat anti-rabbit IgG were used as secondary antibodies, respectively, followed by visualization with liquid diaminobenzidine (DAB) plus chromogen substrate solution (Dako). Sections were counterstained with hemalaun (Merck). For histopathological analyses, sections were stained with Luxol fast blue/periodic acid Schiff agent (LFB/PAS) and Bielschowsky silver impregnation to assess inflammation, demyelination and axonal pathology, respectively. Stained sections were scanned using Pannoramic Digital Slide Scanner 250 FLASH II or P1000 (3DHistech) at ×200 magnification and in a final resolution of 0.22 μm/px.

The meningeal area of $B220^+$ cell aggregates (MEBAGs) and the spinal cord white matter area of the same section were quantified using the 3DHistech Pannoramic Viewer Tool. The MEBAG area was then calculated as fraction of the respective white matter area. For each mouse the three sections with the largest MEBAGs were included, and at least three mice per group were analysed. For quantification of the Mac-3 signal in the spinal cord parenchyma (including white and grey matter but excluding the meningeal compartment), whole slide images were analysed using a custom-made script based on Cognition Network Language (Definiens Developer XD software V2.7.0, Definiens AG). Tissue was detected and only spinal cord sections were further processed. DAB detection was performed using a Bayesian classifier for this stain. For each section, the total parenchymal area and the DAB^+ area within the parenchyma were calculated. Data were summarized using R-project (R Core Team (2014). R: A language and environment for statistical computing. R Foundation for Statistical Computing, Vienna, Austria (http://www.R-project.org/ accessed 12 May 2021).

RNAscope *in situ* hybridization

Fluorescent *in situ* hybridization (FISH) was done using the RNAscope® Fluorescent Multiplex Kit V2 (cat 323100, Advanced Cell

Diagnostics, Inc.). The *in situ* hybridization protocol was performed following recommended specifications for murine FFPE brain tissue. Probes against murine *Ebi3* (cat 448921), *Il10*-C3 (cat 317261-C3) and *Il12a*-C2 (cat 414881-C2) were commercially available from Advanced Cell Diagnostics, Inc. RNAscope. *Ebi3* was visualized by Tyramide Signal Amplification (TSA) plus Fluorescein (Perkin Elmer, NEL741001KT), *Il10*-C3 was visualized with TSA plus Cyanine 3 (Perkin Elmer, NEL744001KT), and *Il12*-C2 was visualized with TSA plus Cyanine 5 (Perkin Elmer, NEL745001KT). The FISH protocol on murine brains was followed by fluorescence immunostaining with rat anti-mouse B220 (eBioscience, clone RA3-6B2) and visualized using a secondary donkey anti-rat IgG (H+L) conjugated with DyLight 405 (Jackson Immunoresearch, Cat. 712-475-153). As indicated in the manufacturer's protocol, positive control probes (Cat. 320881) containing *Polr2a*-C1, *Ppib*-C2, *Ubc*-C3 and negative control probes *DapB* (Cat. 320871) were used. Confocal images of B220 cell clusters were acquired at ×63 magnification (Zeiss LSM800). Positive signals were quantified by a blinded experimenter using ZEN 2.3 lite (Zeiss). For representative images, contrast was linearly enhanced using the tools levels, curves, brightness, and contrast in Adobe Photoshop CC.

Preparation of mononuclear cells from the CNS and flow cytometry

At the peak of disease, CNS-infiltrating cells were isolated after perfusion through the left cardiac ventricle with PBS. Brain and spinal cord were extracted. Tissues were digested with collagenase D (2.5 mg/ml) and DNase I (1 mg/ml) at 37°C for 45 min. After passing the tissue through a 70-μm cell strainer, cells of the spinal cord and brain were separated by discontinuous Percoll® gradient (70%/37%) centrifugation. Mononuclear cells were isolated from the interphase.

Cells were stained with live/dead fixable dyes [Aqua (405 nm excitation), Invitrogen] and antibodies to surface markers: CD3e (145-2C11), CD4 (GK1.5 or RM4-5), CD8α (53–6.7), CD11b (M1/70), CD11c (HL3), CD19 (1D3 or 6D5), CD44 (IM7), CD45 (30-F11), CD45.1 (A20), CD45.2 (104), CD45R (B220; RA3-6B2), CD49d (α4 integrin, 9C10/MFR.4.B), 2D2 TCR Vα3.2 (RR3-16) and Vβ11 (RR3-15); all BD Biosciences, eBioscience or BioLegend.

For intracellular cytokine staining, cells were restimulated with 50 ng/ml PMA (Sigma-Aldrich), 1 μg/ml ionomycin (Sigma-Aldrich) and monensin (1 μl/ml BD GolgiStop) at 37°C for 2.5 h. Subsequent to live/dead and surface staining, cells were fixed and permeabilized (Cytofix/Cytoperm™ and Perm/Wash Buffer; BD Biosciences), and stained for cytokines IL-17A (TC11-18H10.1; BioLegend) and IFN-γ (XMG1.2, eBioscience). Cells were analysed using a CyAn™ ADP 9 flow cytometer (Beckmann/Coulter) and a CytoFLEX S (Beckmann Coulter). Cell counting was performed by a Guava easyCyte 5HT cytometer (Merck) together with 7-AAD (BD), Fixable Red Dead Cell Stain (ThermoFisher), or Fixable Viability Dye eFluor™ 520 (eBioscience) and CD45 (30-F11) or CD45.2 (104). All data analysis was facilitated using FlowJo version 10 (Tree Star, now BD Biosciences).

Quantification and statistical analysis

Statistical evaluations of cell frequency measurements and cell numbers were performed by one-way ANOVA followed by Sidak's multiple comparison test when two genotypes of multiple cell populations were compared, as indicated in the figure legends. Multiplicity adjusted *P*-values < 0.05 were considered significant. EAE scores between groups were analysed as disease burden per individual day with one-way ANOVA and Dunnett's *post hoc* test. Alternatively, the disease burden was calculated as 'area under the curve' and compared by *t*-test between groups, as indicated in the figure legends. Body-weight loss was assessed by two-way ANOVA followed by Sidak's multiple comparisons test. Statistical analysis was performed in Graphpad Prism 8.4.3 (Graphpad Software, Inc).

Data availability

The data that support the findings of this study are available from the corresponding author upon reasonable request.

Results

T cell-conditional ablation of *Itga4* in OSE mice increases the incidence of opticospinal encephalomyelitis

Th17 cells (but not Th1 cells) are able to access the CNS compartment in the absence of *Itga4* or when a blocking antibody to Itga4 is administered in the MOG(35–55)-induced EAE model.[25,26] Similar findings were reported in humans when analysing T helper cell subsets in the blood and the CSF of patients with multiple sclerosis.[26,27]

Here, we used an established model of opticospinal multiple sclerosis, i.e. a double transgenic mouse line expressing a MOG-specific TCR and BCR (termed OSE mice)[16,17] to test the clinical relevance of genetic ablation of *Itga4* on antigen-specific T cells in a model that is independent of adjuvant-mediated immune activation. OSE mice were crossed with *Cd4-Cre* transgenic animals as well as with mice bearing a floxed *Itga4* allele.[18] This breeding yielded T cell-conditional α4 integrin-deficient OSE mice (TCR^{MOG}; $BCR^{MOG,\ KI/KI}$; $Itga4^{flox/flox}$; *Cd4-Cre*), termed OSE-$Itga4^{\Delta T}$ mice. As reported,[17] control OSE mice (TCR^{MOG}; $BCR^{MOG,\ KI/KI}$; $Itga4^{flox/flox}$) developed CNS disease with an incidence of 60% at 6 weeks of age. In contrast, OSE-$Itga4^{\Delta T}$ mice developed disease at a higher incidence than OSE control mice (Fig. 1A). At 6 weeks of age, more than 80% of OSE-$Itga4^{\Delta T}$ mice were sick. We did not observe a predominant 'atypical', i.e. atactic, disease phenotype in OSE-$Itga4^{\Delta T}$ mice, and the mortality and disease course of OSE-$Itga4^{\Delta T}$ mice and regular OSE mice were comparable (Fig. 1B and Supplementary Table 1). Taken together, genetic ablation of *Itga4* in T cells increased the incidence of opticospinal EAE.

OSE-$Itga4^{\Delta T}$ mice exhibit higher numbers of Th17 cells within the CNS parenchyma

To assess the cytokine phenotype of the CNS T cells in this OSE model, we isolated the mononuclear cell infiltrate from the CNS compartment of sick OSE and OSE-$Itga4^{\Delta T}$ mice on Day 20 after disease onset. We found significantly higher numbers of Th17 cells in the CNS of OSE-$Itga4^{\Delta T}$ mice than in the CNS of OSE control mice (Fig. 1C, bottom). Also, the number of IL-17/IFN-γ double producing $CD4^+$ T cells was increased in OSE-$Itga4^{\Delta T}$ mice (Fig. 1C, bottom) while the number of IFN-γ producers was similar in the CNS of OSE-$Itga4^{\Delta T}$ mice and OSE control mice. As the number of Th17 cells in the spleen of OSE-$Itga4^{\Delta T}$ mice and OSE mice was not significantly different (Fig. 1C, top), we concluded that the higher number of Th17 cells in the CNS of OSE-$Itga4^{\Delta T}$ mice was due to a preferential recruitment of Th17 cells to the CNS and not attributable to generalized differences in the commitment of T helper cells in the peripheral immune compartment of OSE and OSE-$Itga4^{\Delta T}$ mice. To test the priming of MOG-specific T cells sufficient and deficient in α4 integrin expression, we transferred naive 2D2 T cells or $Itga4^{-/-}$ 2D2 T cells into BCR^{MOG} transgenic (TH) recipients, challenged them with MOG peptide (in the absence of adjuvant) and tested the indicator cells for proliferation and cytokine production.

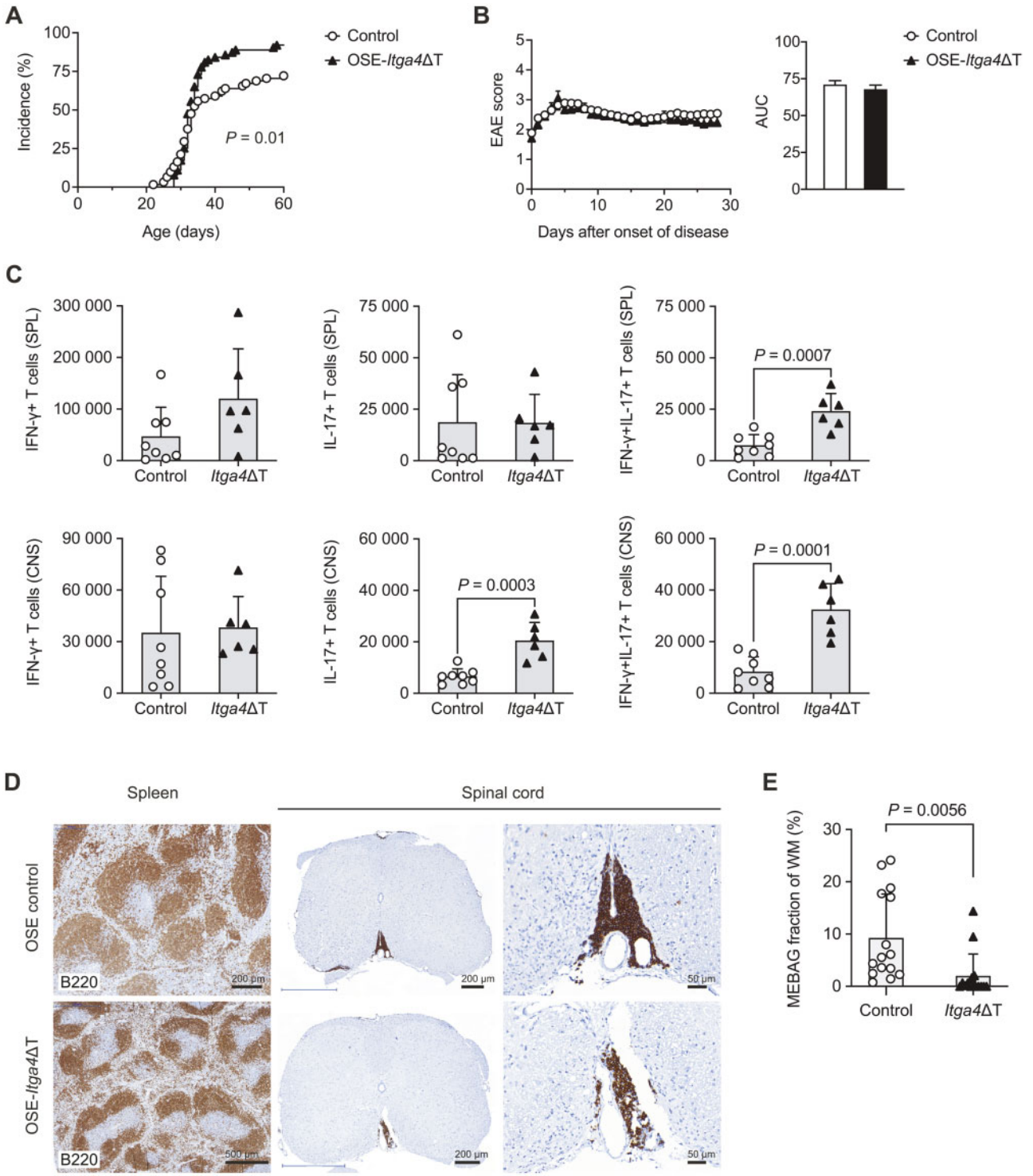

Figure 1 α4 integrin expression on T cells is necessary for the induction of MEBAGs in the OSE mouse model. (**A** and **B**) Spontaneous EAE was monitored in littermate control mice (OSE; TCR^{MOG}; $BCR^{MOG,\ KI/KI}$; $Itga4^{flox/flox}$, n = 68) and T cell-conditional α4 integrin deficient OSE mice (OSE-$Itga4^{\Delta T}$; TCR^{MOG}; $BCR^{MOG,\ KI/KI}$; $Itga4^{flox/flox}$, *Cd4-Cre*, n = 76). (**A**) Incidence of clinical signs of disease; survival curve, Mantel-Cox log-rank test. (**B**) EAE score including area under the curve (AUC), Student's *t*-test. (**C**) Three to 5 days after onset of disease, mononuclear cells were isolated from the spleen and the CNS of diseased OSE and OSE-$Itga4^{\Delta T}$ mice and investigated by intracellular cytokine staining. Absolute numbers of IFN-γ producing $CD4^+$ T cells, of IL-17 producing $CD4^+$ T cells, and of double producers in the spleen (*top row*) and in the CNS (*bottom row*) of OSE control or OSE-$Itga4^{\Delta T}$ mice. Student's *t*-test, symbols indicate individual mice. (**D** and **E**) Immunohistochemical staining for B220 in OSE mice and OSE-$Itga4^{\Delta T}$ mice at 4 weeks after disease onset. (**D**) Representative spinal cord sections. Scale bar = 500 µm, 200 µm, 50 µm. (**E**) The meningeal area covered by MEBAGs was assessed as fraction of the transversal white matter area at the respective spinal cord level. Symbols indicate individual sections. In each group five mice were included in the analysis, and the three sections of each mouse with the largest MEBAGs were analysed; unpaired Student's *t*-test. WM = white matter.

Both the proliferative response as well as the production of IFN-γ and IL-17 were similar in 2D2 T cells and *Itga4*$^{-/-}$ 2D2 T cells, re-isolated from the spleen of TH host mice, indicating that lack of α4 integrin expression in T cells did not push their commitment to the Th17 lineage (Supplementary Fig. 1). Rather, the higher number of Th17 cells in the CNS of OSE-*Itga4*$^{\Delta T}$ mice as compared to OSE mice pointed to a differential recruitment to the CNS. These results are in line with previous reports suggesting that Th17 cells are able to use alternative routes into the CNS independent of α4 integrin expression.[26–28] Notably, even though the OSE-*Itga4*$^{\Delta T}$ model does not rely on immunization with a strong adjuvant that might bias the immune reaction towards a Th17 response, a predominance of antigen-specific Th17 cells was an eminent feature of the CNS T cell compartment in OSE-*Itga4*$^{\Delta T}$ mice.

MEBAGs are decreased in OSE-*Itga4*$^{\Delta T}$ mice

Meningeal B cell aggregates (MEBAGs) have been described in the OSE model.[16,17] These aggregates mostly consist of B cells and exhibit structural and functional features of tertiary lymphoid follicles (for reviews, see Drayton *et al.*[29] and Mitsdoerffer and Peters[30]). However, while correlative data have been published in human multiple sclerosis cases,[1,31] the relevance of meningeal lymphocytic aggregates as to CNS immunopathology and clinical disease course is unclear. Therefore, we analysed the extent of MEBAGs in OSE control mice and OSE-*Itga4*$^{\Delta T}$ mice, which differed in their disease incidence. Control OSE mice showed extensive meningeal lymphocytic aggregates. In contrast, OSE-*Itga4*$^{\Delta T}$ mice had significantly fewer and smaller meningeal lymphocytic infiltrates in relation to the corresponding trans-sectional white matter area (Fig. 1D and E), despite prominent infiltration of the meninges and parenchyma with α4 integrin deficient Th17 cells.

Systemic B cell depletion has disease phase-specific effects in OSE mice

OSE-*Itga4*$^{\Delta T}$ mice suffered from enhanced intrathecal inflammation even though the number of MEBAGs was reduced. To address whether the presence of MEBAGs fed back on intrathecal inflammation, we aimed to acutely eliminate MEBAGs in OSE mice. Since B cells are the primary constituent of MEBAGs, we decided to apply a B cell-depletion strategy. First, we used an anti-CD20 antibody in the presymptomatic stage of wild-type OSE mice. In accordance with prior studies in a spontaneous EAE model,[32] B cell-depletion before the onset of clinical signs resulted in delayed and less severe disease in OSE mice as compared to control antibody treatment (Fig. 2A, B and Supplementary Table 2), consistent with the idea that interference with the APC function of B cells in secondary lymphoid tissues decreases priming of encephalitogenic T cells. In this setting the formation of MEBAGs was not abrogated. However, the area covered by MEBAGs in relation to the trans-sectional white matter area was reduced in OSE mice after presymptomatic anti-CD20 treatment as compared to control-treatment (Fig. 2C and D).

To tease apart the relevance of B cells as APCs in the peripheral immune compartment and in MEBAGs and thus a potential role of B cells in sustained intrathecal inflammation, we used anti-CD20 in OSE mice, only after clinical signs of disease were apparent. In this setting, administration of an anti-CD20 antibody failed to improve the clinical score in OSE mice and by tendency, even worsened the disease burden on the population level (Fig. 3A, B and Supplementary Table 3). While anti-CD20 treatment after onset of disease led to efficient elimination of B cells from the circulation and from peripheral lymph nodes (Supplementary Fig. 2), the area of MEBAGs was not significantly reduced in OSE mice with variable effects of anti-CD20 treatment on established MEBAGs (Fig. 3C and D), indicating that intrathecal MEBAG-resident B cells were relatively resistant to depletion with anti-CD20 antibodies.

In more detailed histological analyses, we observed that post-symptomatic anti-CD20 treatment of OSE mice failed to attenuate inflammatory pathology in the spinal cord of OSE mice. Indeed, inflammatory infiltrates of T cells and macrophages tended to be more widespread into the spinal cord white matter and less restricted to the vicinity of MEBAGs in anti-CD20 treated than in control-treated OSE mice (Fig. 3E), concomitant with an equally widespread demyelination and loss of axonal density (as assessed by LFB-PAS and Bielschowsky staining, respectively; Fig. 3E). Therefore, the histopathological analysis largely mirrored the clinical phenotype and supported the idea that established MEBAGs might have a role in mitigating the deep infiltration of inflammatory cells from the subarachnoid space into the CNS parenchyma.

The ablation of MEBAGs in OSE-*Itga4*$^{\Delta B}$ mice leads to a higher disease burden

It has previously been reported that the recruitment of B cells to the meningeal compartment is entirely dependent on the expression of α4 integrins on B cells while ablation of *Itga4* on B cells does not affect the 'immune function' of B cells in the systemic compartment.[33] Therefore, we wanted to test whether ablation of *Itga4* on B cells could be used as a means to manipulate the formation of MEBAGs without interfering with systemic immune functions of B cells in the OSE model. We crossed CD19-Cre$^{KI/wt}$ into the OSE background that carried floxed alleles of *Itga4* (TCR^{MOG}; BCR$^{MOG, KI/KI}$; *Itga4*$^{flox/flox}$; *Cd19-Cre*$^{KI/wt}$) and termed these B cell-conditional α4 integrin deficient OSE animals OSE-*Itga4*$^{\Delta B}$ mice. First, cohorts of OSE-*Itga4*$^{\Delta B}$ and littermate control mice (TCR^{MOG}; BCR$^{MOG, KI/KI}$; *Itga4*$^{flox/flox}$; *Cd19-Cre*$^{wt/wt}$) were monitored for their clinical disease course. Over extended observation periods, the incidence was similar, but the disease burden and mortality were higher in OSE-*Itga4*$^{\Delta B}$ mice than in control animals (Fig. 4A–C). As expected, the meningeal infiltrates in OSE-*Itga4*$^{\Delta B}$ mice were essentially devoid of B cells and by definition, the area of MEBAGs in these mice was significantly reduced as compared to littermate controls (Fig. 4D and E). In histological analyses, we noticed that the depth of infiltrates of T cells and macrophages from the meningeal surface into the spinal cord white matter as well as the subsequent demyelination were increased in OSE-*Itga4*$^{\Delta B}$ mice as compared to regular OSE control mice (Fig. 4F and G). These results supported the notion that B cells in MEBAGs might adopt an immunomodulatory function during sustained CNS inflammation.

Anti-CD19 CAR-T cells mediate efficient interventional depletion of B cells in MEBAGs

While OSE-*Itga4*$^{\Delta B}$ mice never developed MEBAGs, from a 'therapeutic' perspective the acute depletion of already established MEBAGs is a more relevant intervention, and we have observed that anti-CD20 antibody administration failed to efficiently ablate established MEBAGs in OSE mice (Fig. 3). Therefore, we explored alternative methods to deplete MEBAG-resident B cells. Here, we tested an anti-CD19 CAR-T cell approach that had been used in a preclinical model for acute lymphoblastic leukaemia.[21] Because of their higher density of MEBAGs as compared to OSE-*Itga4*$^{\Delta T}$ mice, we used regular OSE mice for the CAR-T cell experimental design. Since CAR-T cell recipients needed to be sublethally irradiated in order to increase the take-rate of transferred cells, we first investigated the impact of this irradiation protocol (see 'Materials and methods' section) on the natural disease course of OSE mice and confirmed that sublethal irradiation of OSE mice reduced but

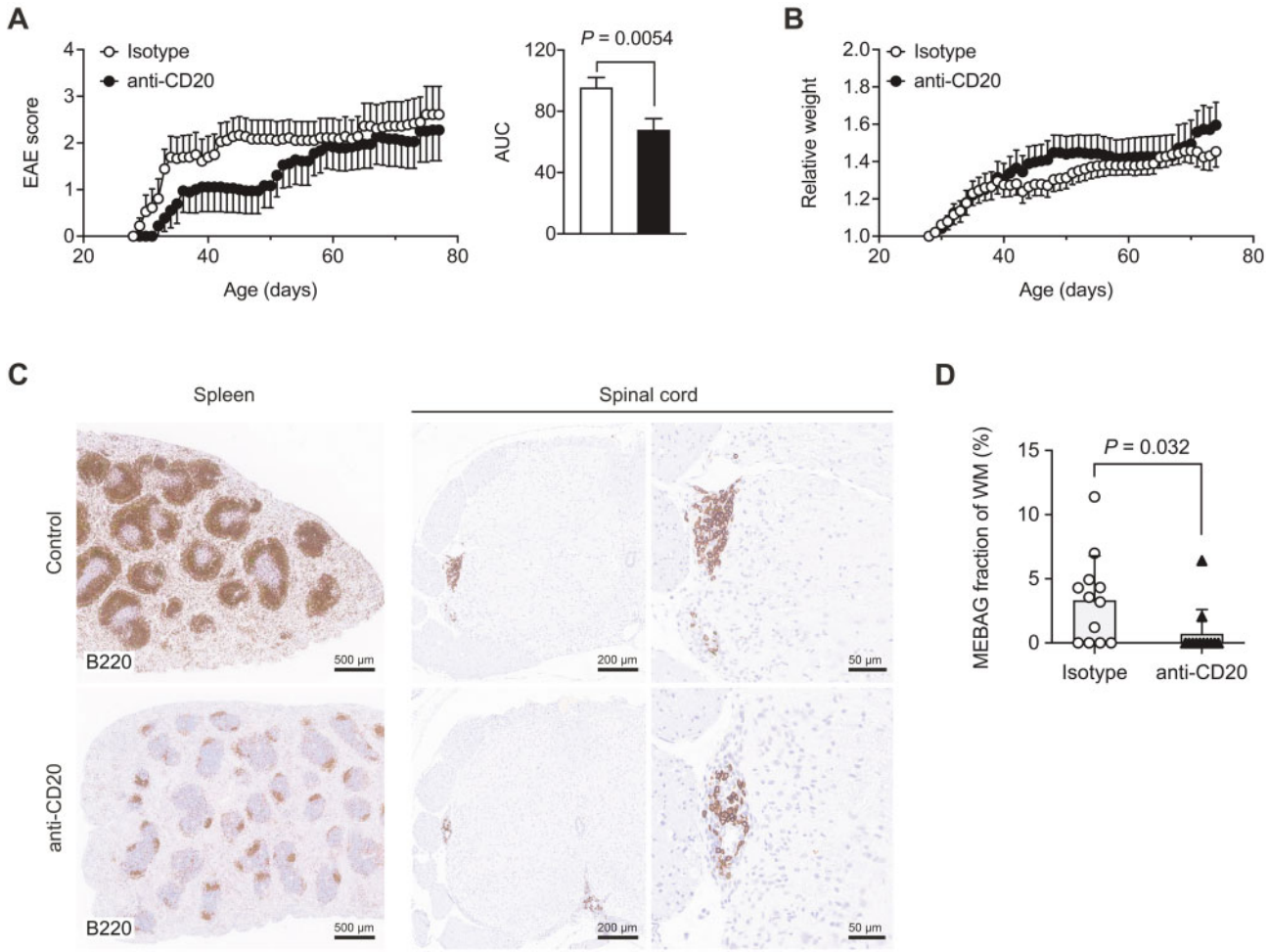

Figure 2 Pre-onset depletion of B cells delays and attenuates spontaneous EAE but does not prevent chronic progressive disease. OSE mice were either treated with isotype control antibody or with a depleting anti-mouse CD20 monoclonal antibody (18B12, IgG1), throughout the experiment starting at 4 weeks of age. Isotype (IgG1), $n = 9$; anti-CD20, $n = 9$. (**A**) EAE score including AUC, Student's *t*-test. (**B**) Relative weight. (**C**) At the end of the clinical monitoring period, spleen and spinal cord sections were analysed for B cells by staining with B220. Representative sections for isotype control or anti-CD20 treated mice, respectively. Scale bars = 500 µm, 200 µm, 50 µm. (**D**) The MEBAG area was assessed as fraction of the transversal white matter area at the respective spinal cord level. Symbols indicate individual sections. In each group four mice were included in the analysis, and the three sections of each mouse with the largest MEBAGs were analysed; unpaired Student's *t*-test.

did not prevent the development of progressive disease (Supplementary Fig. 3). Next, sublethally irradiated OSE mice received either control cells or anti-CD19 CAR-T cells. In contrast to systemic anti-CD20 treatment, B cells in tissues including in MEBAGs were substantially depleted in anti-CD19 CAR-T cell recipients as compared to control-treated OSE mice when analysed at 3 weeks after anti-CD19 CAR-T cell administration (Fig. 5A and B). The administration of anti-CD19 CAR-T cells was not associated with a gross disruption of the blood–brain barrier in our model (Supplementary Fig. 4), even though it has been reported that anti-CD19 CAR-T cells might have off-target effects on a small subfraction of pericytes in C57BL/6 mice.[34] Notably, during a latency period of ~2 weeks, anti-CD19 CAR-T cell treatment did not alter the clinical course in OSE mice as compared to control-treated mice (Fig. 5C and Supplementary Table 4), suggesting that this intervention was not associated with a substantial cytokine storm. However, as of 2 weeks post administration, anti-CD19 CAR-T cell recipients developed a more severe disease course with marked lethality as compared with their control counterparts (Fig. 5C and Supplementary Table 4). While MEBAGs were strongly reduced or ablated in these mice, anti-CD19 CAR-T cell recipients but not control-treated OSE mice, showed massive inflammatory infiltrates of T cells and macrophages that were no longer restricted to the meningeal compartment but were scattered deep into the spinal cord white matter throughout the spinal cord parenchyma (Fig. 5D and E), associated with more widespread demyelination and axonal loss (Fig. 5D). While these data again indicate that MEBAGs might exert an immune regulatory function, this function is mechanistically not well understood. When we tested MEBAGs in regular OSE mice for the expression of *Il10* and *Il35* (*Il12a* plus *Ebi3*) by RNAscope® (Supplementary Fig. 5), the mRNA of these cytokines was clearly associated with B cells in MEBAGs of OSE mice (Fig. 6A–C). In fact, ~10% of MEBAG B cells contained only *Il10* mRNA or *Il35* mRNA, respectively, and an additional 10% expressed both mRNA species. Therefore, one-third of the B cells located in MEBAGs had the potential to produce these immunomodulatory cytokines (Fig. 6D)—a feature that was entirely lost with the extensive ablation of MEBAGs after anti-CD19 CAR-T cell treatment.

In summary, our data suggest that B cell depletion with a monoclonal antibody to CD20 will only insufficiently target

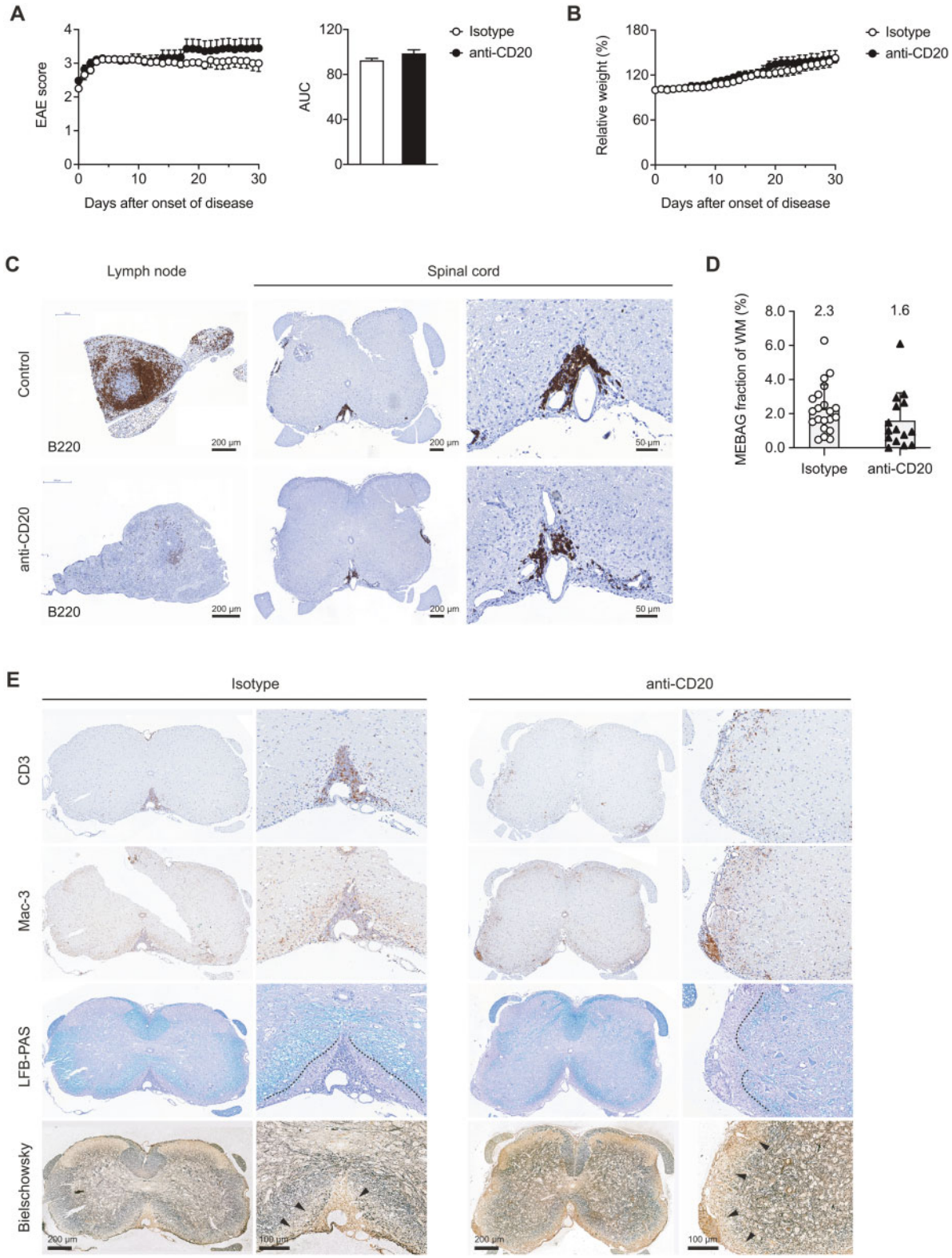

Figure 3 Post-onset depletion of B cells fails to improve clinical signs of disease. (**A** and **B**) OSE mice were treated with isotype control antibody (IgG1) or a depleting antibody to CD20. Treatment (injection of 10 µg/g body weight of isotype antibody or anti-CD20 intraperitoneally once a week) was initiated when an individual mouse reached a score of 2 and continued throughout the experiment. (**A**) EAE score including AUC, Student's *t*-test. (**B**) Relative weight. (**C**) Immunohistochemical analysis for B220 (staining B cells) in lymph node and spinal cord sections prepared at 4 weeks after start of treatment of OSE mice as indicated. Representative sections. Scale bars = 200 µm and 50 µm. (**D**) The meningeal area covered by MEBAGs was assessed as fraction of the transversal white matter area at the respective spinal cord level of OSE mice analysed at 4 weeks after start of treatment with control antibody or anti-CD20. Multiple sections of at least three mice per group; unpaired Student's *t*-test. (**E**) Representative spinal cord sections stained for T cells (CD3) and macrophages (Mac-3) of OSE mice treated post-EAE-onset with control IgG1 or anti-CD20. Note that the demyelinated area (limited by dashed line in the LFB-PAS stainings) and the area of reduced axonal density (arrow heads in the Bielschowsky stainings) largely corresponded to the intensity of the macrophage infiltrate in each condition. Scale bars = 200 µm and 100 µm. WM = white matter.

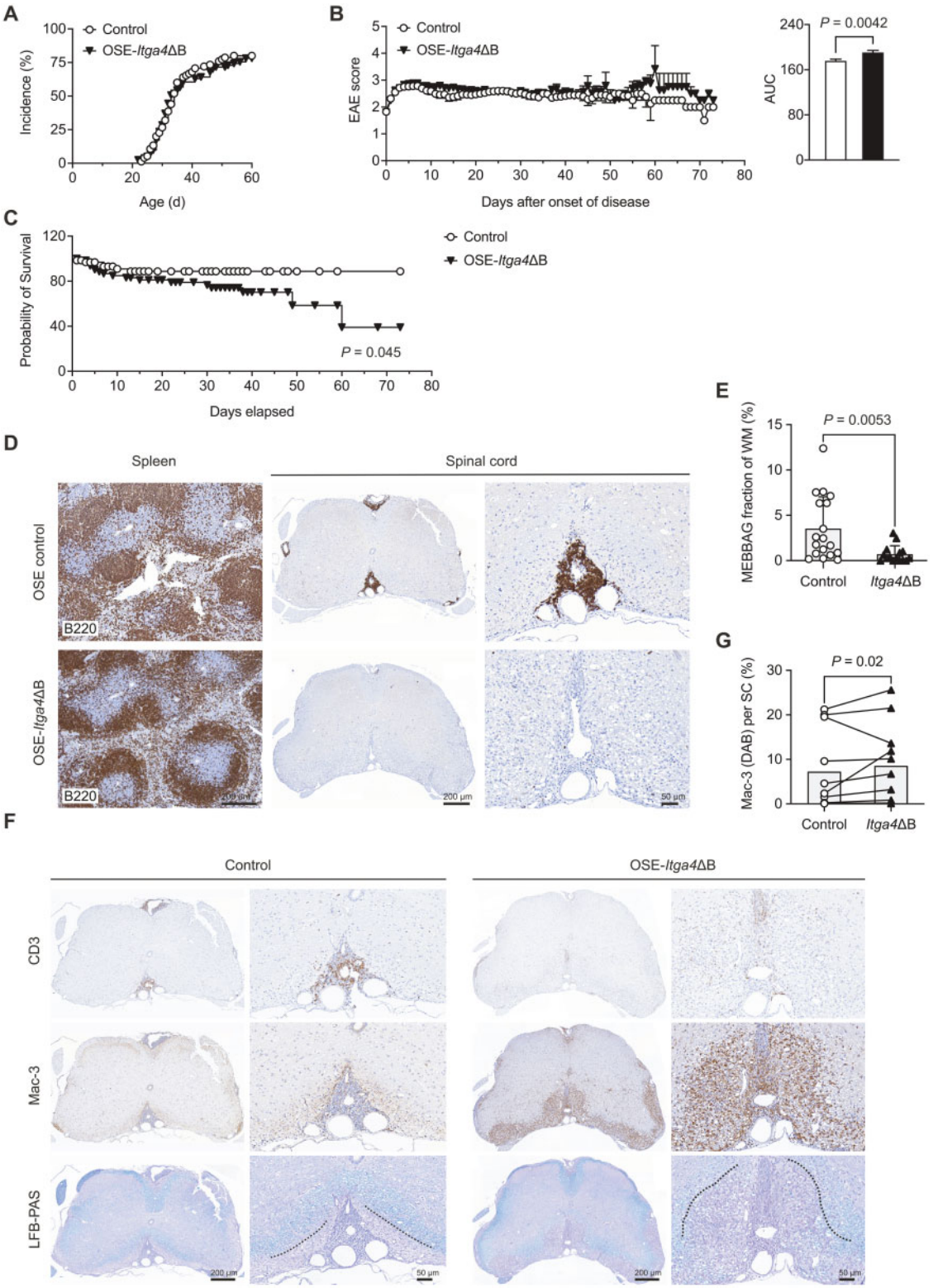

Figure 4 OSE-*Itga4*$^{\Delta B}$ mice fail to build up MEBAGs in the spinal cord meningeal compartment and show a pronounced disease burden. Spontaneous EAE was monitored in littermate control mice (OSE; TCR^{MOG}; BCR$^{MOG,\ KI/KI}$; *Itga4*$^{flox/flox}$, n = 68) and B cell-conditional α4 integrin deficient OSE mice (OSE-*Itga4*$^{\Delta B}$; TCR^{MOG}; BCR$^{MOG,\ KI/KI}$; *Itga4*$^{flox/flox}$, *Cd19-Cre*$^{wt/KI}$, n = 76). **(A)** Incidence of EAE in OSE and OSE-*Itga4*$^{\Delta B}$ mice. **(B)** EAE score including AUC, Student's *t*-test. **(C)** Mortality of OSE and OSE-*Itga4*$^{\Delta B}$ mice; Mantel-Cox log-rank test. **(D)** In some animals, spleen and spinal cord sections were analysed for B cells by staining with B220 at around 4 weeks after onset of disease. Representative sections for OSE control or OSE-*Itga4*$^{\Delta B}$ mice, respectively. Scale bars = 200 μm and 50 μm. **(E)** The MEBAG area was assessed as fraction of the transversal white matter area at the respective spinal cord level. Symbols indicate individual sections. In each group six mice were included in the analysis, and the three sections of each mouse with the largest MEBAGs were analysed; unpaired Student's *t*-test. **(F)** Spinal cord sections of OSE control mice or OSE-*Itga4*$^{\Delta B}$ mice were prepared 4 weeks after onset of disease and stained for T cells (CD3) and macrophages (Mac-3). The amount of demyelination was assessed by LFB-PAS (demyelinated area limited by dashed line). Scale bars = 200 μm and 50 μm. **(G)** The macrophage infiltrate in the spinal cord parenchyma was quantified in littermate control mice and OSE-*Itga4*$^{\Delta B}$ mice by assessing the fraction of the spinal cord parenchyma (excluding meninges) that displayed a Mac-3 signal. Individual mice from the two groups were paired, and the spinal cord sections with the largest Mac-3 infiltrates from three mice in each group were analysed. Bars represent means; *t*-test.

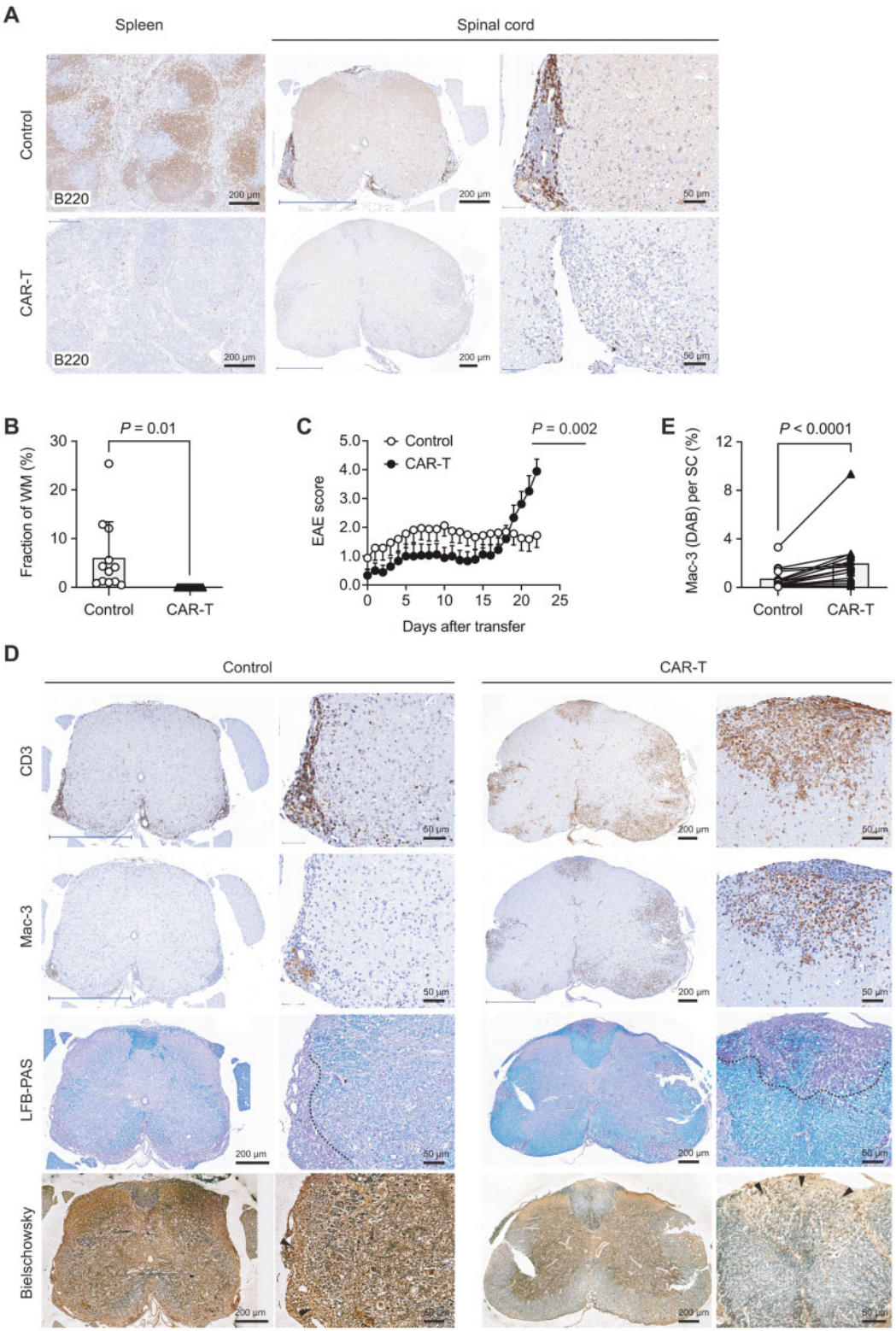

Figure 5 Anti-CD19 CAR-T cell intervention eliminates MEBAGs and is associated with delayed worsening of disease in OSE mice. After sublethal irradiation, OSE mice were monitored for clinical signs of EAE. At first signs of EAE, mice were either transferred with control cells or with T cells that were engineered to express an anti-CD19 CAR construct. (**A**) Three weeks after transfer, the elimination of B cells in various compartments was analysed by immunohistochemistry. B220 staining in spleen (*left*) and spinal cord meninges (*middle* and *right*). Representative sections of control-treated (*top row*) and anti-CD19 CAR-T cell treated (*bottom row*) OSE mice. Scale bar = 200 µm and 50 µm. (**B**) The MEBAG area in control cell-treated and CAR-T cell-treated mice was assessed as fraction of the transversal white matter area at the respective spinal cord level. Symbols indicate individual sections. In each group at least three mice were included in the analysis, and the three sections of each mouse with the largest MEBAGs were analysed; unpaired Student's *t*-test. (**C**) EAE score of control-treated (n = 8) versus anti-CD19 CAR-T cell-treated (n = 9) OSE mice. ANOVA plus Sidak's post-test for individual days. Representative of two experiments. (**D**) Immunohistochemical analysis of T cell (CD3, *top row*) and macrophage (Mac-3) infiltrates into the spinal cord as well as demyelination (LFB-PAS) and axonal density (Bielschowsky) in spinal cord sections of control-treated OSE mice (*left*) and anti-CD19 CAR-T cell-treated OSE mice (*right*) on Day 23 after start of treatment. Scale bar = 200 µm and 50 µm. (**E**) The macrophage infiltrate in the spinal cord parenchyma (excluding meninges) of control-treated and anti-CD19 CAR-T cell-treated OSE mice was assessed by pairing individual mice of each group. The spinal cord sections with the top five largest Mac-3 infiltrates of three mice in each group were analysed. Bars represent means; *t*-test. SC = spinal cord; WM = white matter.

MEBAGs. In contrast, when MEBAGs are ablated by anti-CD19 CAR-T cell administration, the inflammatory response in the CNS compartment is fundamentally exacerbated, implying a regulatory role of MEBAGs. Consistent with this finding, OSE-*Itga4*$^{\Delta B}$ mice that essentially lack MEBAGs in the first place build up an enhanced intrathecal inflammatory load.

Discussion

In this study, we introduce several strategies to modulate the formation of meningeal lymphocyte aggregates in a model of spontaneous CNS autoimmunity. By ablating α4 integrins on MOG-specific T cells or on MOG-specific B cells, severe inflammation in the CNS was uncoupled from the formation of MEBAGs in OSE mice. Similarly, in wild-type OSE mice with a build-up of MEBAGs, anti-CD19 CAR-T cell-mediated elimination of B cells efficiently reduced the amount of MEBAGs but aggravated disease progression. Our data suggest that (i) the formation of meningeal lymphocyte aggregates is associated with a progressive phenotype in a spontaneous mouse model of EAE; (ii) firm establishment of meningeal lymphocyte aggregates marks a stage of the disease where antibody mediated immune interventions in the systemic immune compartment fail to decrease inflammation within the CNS; and (iii) MEBAGs might have a regulatory function during chronic inflammation in the meningeal compartment.

Th17 cells have been shown to be inducers of ectopic lymphoid tissue in the meningeal compartment.[10] Our data appear to contrast this observation since OSE-*Itga4*$^{\Delta T}$ mice had fewer and smaller MEBAGs despite extensive Th17 driven inflammation in the CNS. However, in our model, Th17 cells lacked α4 integrin expression, and our data suggest that α4 integrin expression on T cells in the intrathecal compartment is directly involved in the

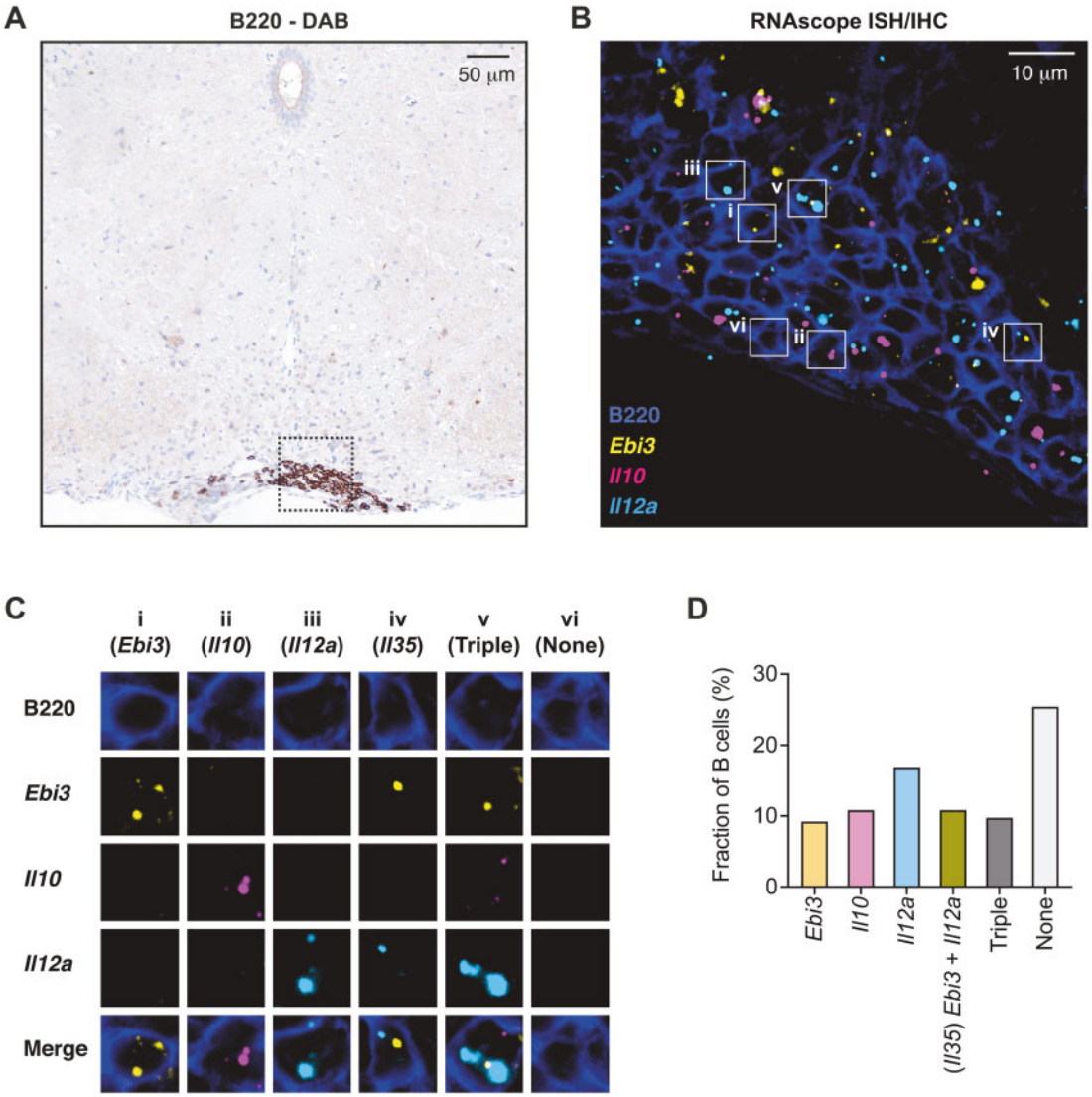

Figure 6 B cells in MEBAGs have the potential to produce immunomodulatory cytokines. Spinal cord sections of untreated OSE mice were prepared three weeks after first manifestation of clinical signs of disease. (**A**) Immunohistochemical staining for B220 to show a representative MEBAG. Scale bar = 50 μm. (**B**) FISH was performed using the RNAscope® protocol for the indicated probes, and a representative MEBAG (as outlined in **A**) is depicted. Scale bar = 10 μm. (**C**) Magnification of individual B cells as identified by B220 staining (**i–vi**) as indicated in **B**, stained for the RNA species *Ebi3*, *Il10*, and *Il12a* by RNAscope®. (**D**) Quantification of B cells positive for the indicated RNA species. Fraction of RNA positive B cells of all B cells within MEBAGs. Analysis of *n* = 6 MEBAGs from three mice. ISH/IHC = *in situ* hybridization/immunohistochemistry.

formation of MEBAGs. A putative role of α4 integrins has been suggested in lymphoid tissue inducer cells, which are instrumental in the formation of ectopic lymphoid tissue in distinct niches in the gut during development[35] and in restoration of secondary lymphoid tissue architecture after infection in adults.[36] Here, we exploited our observation of reduced MEBAG formation in the CNS compartment in OSE-*Itga4*$^{\Delta T}$ mice to investigate the functional significance of MEBAGs for immunopathology during CNS autoimmunity.

Compelling evidence suggests that CD20-targeted B cell-depleting therapeutic interventions are highly efficient in patients with relapsing multiple sclerosis.[37,38] Similarly, depletion of B cells before disease onset in a model, in which a MOG-specific TCR was transgenically expressed on an SJL genetic background, prevented spontaneous EAE,[32] suggesting that cognate B cells might be powerful (and perhaps indispensable) antigen presenting cells to autoreactive T cells in the systemic immune compartment.[39] Our results in the OSE model confirmed this observation because preemptive B cell depletion by a monoclonal antibody to CD20 delayed the onset and mitigated the clinical signs of disease. Conversely, in the OSE-*Itga4*$^{\Delta B}$ model, in which the systemic APC function of B cells was likely unaltered but lacked MEBAGs, the initial phase of EAE was identical to regular OSE mice. However, over time the disease burden of OSE-*Itga4*$^{\Delta B}$ mice was higher than in OSE controls, which correlated with a more pronounced inflammatory tissue damage in the absence of MEBAGs in OSE-*Itga4*$^{\Delta B}$ mice.

Interestingly, in humans, where anti-CD20 therapy is highly efficient in limiting systemic inflammatory activity in patients with multiple sclerosis, secondary progression of disease may not be prevented[40] (even though larger scale trials to investigate this observation systematically are lacking). The rationale for the application of B cell targeted therapies in progressive stages of multiple sclerosis has been built on the observation that B cells constitute a major cellular component of the meningeal infiltrates that were observed in multiple sclerosis patients with chronic disease. Correlative data (mostly from human autopsy material) implied that MEBAGs are associated with progressive disease.[1,2,31,41,42] However, while cortical demyelination has been observed in both multiple sclerosis and anti-MOG antibody associated disease,[43] the latter is characterized by the lack of a progressive disease course,[44] and subpial cortical demyelination is also observed in early multiple sclerosis in the absence of high degree meningeal inflammation[45] (for a review see Lassmann[46]). Therefore, the causal pathogenic relevance of MEBAGs remains controversial. In addition, regulatory functions of B cells and plasma cells in the meninges have been identified that rely on the secretion of downmodulatory cytokines such as IL-10.[47] IL-10 producing regulatory B cells and IgA$^+$ plasma cells were shown to be recruited into the subarachnoid space from the systemic immune compartment.[8] Therefore, based on the available data in human patients, it is difficult to conclude that MEBAGs are universal drivers of immunopathology. Apart from these pathophysiological arguments, we need to consider that it is not clear whether antibody-mediated depletion of B cells is at all an efficient means to target inflammatory lymphocyte aggregates in the subarachnoid space.[48,49]

CAR-T cell approaches that target CD19$^+$ B cells are becoming established therapies for certain hematopoietic malignancies (for review see Neepalu *et al.*[50]). Cytokine release syndrome and the so-called immune cell associated neurotoxicity syndrome are early and late complications of this therapy, respectively. However, next generation CAR-T cell approaches will combine their efficient B cell depleting properties with the possibility to re-eliminate the transferred CAR-T cells on demand.[21] Therefore, we considered this strategy in order to deplete tissue resident B cells (within MEBAGs). We used this approach as a tool to investigate the relevance of B cell aggregates in a model of chronic CNS autoimmunity. Anti-CD19 CAR-T cell-mediated depletion of B cells in OSE mice efficiently and (in contrast to anti-CD20 treatment) sustainably reduced MEBAGs, and resulted in an enhanced progressive disease course (due to unleashed inflammation) after a delay of 2 weeks. This delayed worsening is not compatible with a cytokine release syndrome and rather argues in favour of a loss-of-function effect of MEBAGs.

While our data are consistent with the idea that MEBAGs contribute to the local generation of regulatory immune cells, the mechanistic underpinning and compartment-specific steps of this process need to be determined. Notably, even in human autopsy material, MEBAGs were associated with cortical grey matter lesions (with strong microglia and macrophage activation) but also with partially de- and remyelinated cortical lesions. Furthermore, the extent of cortical demyelination did not correlate with the presence of MEBAGs,[51] and therefore, it is possible that MEBAGs would not so much promote immunopathology in grey matter as they would foster a milieu that enables reparative processes.

A caveat in the translation of our model to the human situation is that meningeal pathology in OSE mice is focused on the spinal cord meningeal compartment. Adjacent to MEBAGs in OSE mice is the spinal cord white matter as opposed to cortical grey matter in secondary progressive multiple sclerosis patients with forebrain meningeal tertiary lymphoid follicle-like structures. It is likely that white matter and grey matter deal differently with adjacent inflammation. Cortical grey matter tends to support less immune cell infiltrates, resolves inflammation faster and shows a higher propensity to remyelinate.[52,53] Also, MEBAG-produced immunoglobulins and their complement-mediated effector functions might be more harmful to grey matter than to white matter. In our study, we have not addressed antibody secreting functions of MEBAGs and the potential contribution of intrathecally synthesized anti-MOG antibodies or other toxic mediators that have been suggested to contribute to cortical pathology.[54–56] However, by applying an efficient interventional setup to eliminate MEBAGs in a chronic EAE model, our study challenges the view that meningeal lymphocyte aggregates are exclusively drivers of pathogenicity in the CNS. Further mechanistic studies need to consider that these structures might also subserve an effort of the meningeal space to confine chronic inflammation and to reduce immunopathology in the CNS parenchyma. Observations on the failure of therapeutic approaches that targeted BAFF in patients with multiple sclerosis might help to better inform these studies. In fact, neutralizing the plasma cell differentiation and growth factor BAFF aggravated the severity of multiple sclerosis, indicating that B cells might have regulatory properties.[5] The identification of IL-10 and IL-35 in B cells within MEBAGs supports this idea.

Acknowledgements

We would like to thank Tanja Kuhlmann (Institute for Neuropathology, University of Muenster) for help with initial immunohistochemistry stainings.

Funding

T.K. is supported by the Deutsche Forschungsgemeinschaft [SFB1054-B06, TRR128-A07, TRR128-A12, TRR274-A01, and EXC 2145 (SyNergy) ID 390857198], the ERC (CoG 647215), and by the Hertie Network of Clinical Neuroscience. M.M. was supported by the Deutsche Forschungsgemeinschaft [EXC 2145 (Synergy)]. D.M. is supported by the Swiss National Science Foundation (310030_185321) and the ERC (CoG 865026).

Competing interests

The authors report no competing interests.

Supplementary material

Supplementary material is available at *Brain* online.

References

1. Magliozzi R, Howell O, Vora A, et al. Meningeal B-cell follicles in secondary progressive multiple sclerosis associate with early onset of disease and severe cortical pathology. *Brain*. 2007;130: 1089–1104.
2. Howell OW, Reeves CA, Nicholas R, et al. Meningeal inflammation is widespread and linked to cortical pathology in multiple sclerosis. *Brain*. 2011;134:2755–2771.
3. Takemori T, Kaji T, Takahashi Y, Shimoda M, Rajewsky K. Generation of memory B cells inside and outside germinal centers. *Eur J Immunol*. 2014;44:1258–1264.
4. Mackay F, Browning JL. BAFF: a fundamental survival factor for B cells. *Nat Rev Immunol*. 2002;2:465–475.
5. Kappos L, Hartung H-P, Freedman MS, et al.; ATAMS Study Group. Atacicept in multiple sclerosis (ATAMS): A randomised, placebo-controlled, double-blind, phase 2 trial. *Lancet Neurol*. 2014;13:353–363.
6. Mizoguchi A, Mizoguchi E, Takedatsu H, Blumberg RS, Bhan AK. Chronic intestinal inflammatory condition generates IL-10-producing regulatory B cell subset characterized by CD1d upregulation. *Immunity*. 2002;16:219–230.
7. Shen P, Roch T, Lampropoulou V, et al. IL-35-producing B cells are critical regulators of immunity during autoimmune and infectious diseases. *Nature*. 2014;507:366–370.
8. Rojas OL, Pröbstel A-K, Porfilio EA, et al. Recirculating intestinal IgA-producing cells regulate neuroinflammation via IL-10. *Cell*. 2019;176:610–624.e18.
9. Pikor NB, Astarita JL, Summers-Deluca L, et al. Integration of Th17- and lymphotoxin-derived signals initiates meningeal-resident stromal cell remodeling to propagate neuroinflammation. *Immunity*. 2015;43:1160–1173.
10. Peters A, Pitcher LA, Sullivan JM, et al. Th17 cells induce ectopic lymphoid follicles in central nervous system tissue inflammation. *Immunity*. 2011;35:986–996.
11. Yoshida H, Kawamoto H, Santee SM, et al. Expression of alpha(4)beta(7) integrin defines a distinct pathway of lymphoid progenitors committed to T cells, fetal intestinal lymphotoxin producer, NK, and dendritic cells. *J Immunol*. 2001;167: 2511–2521.
12. Magliozzi R, Columba-Cabezas S, Serafini B, Aloisi F. Intracerebral expression of CXCL13 and BAFF is accompanied by formation of lymphoid follicle-like structures in the meninges of mice with relapsing experimental autoimmune encephalomyelitis. *J Neuroimmunol*. 2004;148:11–23.
13. Molnarfi N, Schulze-Topphoff U, Weber MS, et al. MHC class II-dependent B cell APC function is required for induction of CNS autoimmunity independent of myelin-specific antibodies. *J Exp Med*. 2013;210:2921–2937.
14. Bettelli E, Pagany M, Weiner HL, Linington C, Sobel RA, Kuchroo VK. Myelin oligodendrocyte glycoprotein-specific T cell receptor transgenic mice develop spontaneous autoimmune optic neuritis. *J Exp Med*. 2003;197:1073–1081.
15. Litzenburger T, Fässler R, Bauer J, et al. B lymphocytes producing demyelinating autoantibodies: Development and function in gene-targeted transgenic mice. *J Exp Med*. 1998;188: 169–180.
16. Bettelli E, Baeten D, Jäger A, Sobel RA, Kuchroo VK. Myelin oligodendrocyte glycoprotein-specific T and B cells cooperate to induce a Devic-like disease in mice. *J Clin Invest*. 2006;116:2393–2402.
17. Krishnamoorthy G, Lassmann H, Wekerle H, Holz A. Spontaneous opticospinal encephalomyelitis in a double-transgenic mouse model of autoimmune T cell/B cell cooperation. *J Clin Invest*. 2006;116:2385–2392.
18. Scott LM, Priestley GV, Papayannopoulou T. Deletion of alpha4 integrins from adult hematopoietic cells reveals roles in homeostasis, regeneration, and homing. *Mol Cell Biol*. 2003;23: 9349–9360.
19. Lee PP, Fitzpatrick DR, Beard C, et al. A critical role for Dnmt1 and DNA methylation in T cell development, function, and survival. *Immunity*. 2001;15:763–774.
20. Rickert RC, Roes J, Rajewsky K. B lymphocyte-specific, Cre-mediated mutagenesis in mice. *Nucleic Acids Res*. 1997;25: 1317–1318.
21. Paszkiewicz PJ, Fräßle SP, Srivastava S, et al. Targeted antibody-mediated depletion of murine CD19 CAR T cells permanently reverses B cell aplasia. *J Clin Invest*. 2016;126:4262–4272.
22. Wang X, Chang W-C, Wong CW, et al. A transgene-encoded cell surface polypeptide for selection, in vivo tracking, and ablation of engineered cells. *Blood*. 2011;118:1255–1263.
23. Korn T, Mitsdoerffer M, Croxford AL, et al. IL-6 controls Th17 immunity in vivo by inhibiting the conversion of conventional T cells into Foxp3+ regulatory T cells. *Proc Natl Acad Sci U S A*. 2008;105:18460–18465.
24. Knier B, Hiltensperger M, Sie C, et al. Myeloid-derived suppressor cells control B cell accumulation in the central nervous system during autoimmunity. *Nat Immunol*. 2018;19:1341–1351.
25. Glatigny S, Duhen R, Oukka M, Bettelli E. Cutting edge: Loss of α4 integrin expression differentially affects the homing of Th1 and Th17 cells. *J Immunol*. 2011;187:6176–6179.
26. Rothhammer V, Heink S, Petermann F, et al. Th17 lymphocytes traffic to the central nervous system independently of α4 integrin expression during EAE. *J Exp Med*. 2011;208:2465–2476.
27. Schneider-Hohendorf T, Rossaint J, Mohan H, et al. VLA-4 blockade promotes differential routes into human CNS involving PSGL-1 rolling of T cells and MCAM-adhesion of TH17 cells. *J Exp Med*. 2014;211:1833–1846.
28. Reboldi A, Coisne C, Baumjohann D, et al. C-C chemokine receptor 6-regulated entry of TH-17 cells into the CNS through the choroid plexus is required for the initiation of EAE. *Nat Immunol*. 2009;10:514–523.
29. Drayton DL, Liao S, Mounzer RH, Ruddle NH. Lymphoid organ development: From ontogeny to neogenesis. *Nat Immunol*. 2006; 7:344–353.
30. Mitsdoerffer M, Peters A. Tertiary lymphoid organs in central nervous system autoimmunity. *Front. Immun*. 2016;7:451.
31. Magliozzi R, Howell OW, Reeves C, et al. A Gradient of neuronal loss and meningeal inflammation in multiple sclerosis. *Ann Neurol*. 2010;68:477–493.
32. Pöllinger B, Krishnamoorthy G, Berer K, et al. Spontaneous relapsing-remitting EAE in the SJL/J mouse: MOG-reactive transgenic T cells recruit endogenous MOG-specific B cells. *J Exp Med*. 2009;206:1303–1316.
33. Lehmann-Horn K, Sagan SA, Bernard CCA, Sobel RA, Zamvil SS. B-cell very late antigen-4 deficiency reduces leukocyte recruitment and susceptibility to central nervous system autoimmunity. *Ann Neurol*. 2015;77:902–908.
34. Parker KR, Migliorini D, Perkey E, et al. Single-cell analyses identify brain mural cells expressing CD19 as potential off-tumor targets for CAR-T immunotherapies. *Cell*. 2020;183:126–142.e17.
35. Mebius RE. Organogenesis of lymphoid tissues. *Nat Rev Immunol*. 2003;3:292–303.

36. Scandella E, Bolinger B, Lattmann E, et al. Restoration of lymphoid organ integrity through the interaction of lymphoid tissue–inducer cells with stroma of the T cell zone. *Nat Immunol*. 2008; 9:667–675.
37. Hauser SL, Waubant E, Arnold DL, et al. B-cell depletion with rituximab in relapsing-remitting multiple sclerosis. *N Engl J Med*. 2008;358:676–688.
38. Sabatino JJ, Pröbstel A-K, Zamvil SS. B cells in autoimmune and neurodegenerative central nervous system diseases. *Nat Rev Neurosci*. 2019;20:728–745.
39. Häusser-Kinzel S, Weber MS. The role of B cells and antibodies in multiple sclerosis, neuromyelitis optica, and related disorders. *Front. Immun*. 2019;10:201.
40. von Büdingen HC, Bischof A, Eggers EL, et al. Onset of secondary progressive MS after long-term rituximab therapy - a case report. *Ann Clin Transl Neurol*. 2017;4:46–52.
41. Kutzelnigg A, Lucchinetti CF, Stadelmann C, et al. Cortical demyelination and diffuse white matter injury in multiple sclerosis. *Brain*. 2005;128:2705–2712.
42. Reali C, Magliozzi R, Roncaroli F, Nicholas R, Howell OW, Reynolds R. B cell rich meningeal inflammation associates with increased spinal cord pathology in multiple sclerosis. *Brain Pathol*. 2020;30:779–793.
43. Juryńczyk M, Jacob A, Fujihara K, Palace J. Myelin oligodendrocyte glycoprotein (MOG) antibody-associated disease: Practical considerations. *Pract Neurol*. 2019;19:187–195.
44. Juryńczyk M, Messina S, Woodhall MR, et al. Clinical presentation and prognosis in MOG-antibody disease: A UK study. *Brain*. 2017;140:3128–3138.
45. Lucchinetti CF, Popescu BFG, Bunyan RF, et al. Inflammatory cortical demyelination in early multiple sclerosis. *N Engl J Med*. 2011;365:2188–2197.
46. Lassmann H. Pathogenic mechanisms associated with different clinical courses of multiple sclerosis. *Front. Immun*. 2018;9:3116.
47. Magliozzi R, Howell OW, Nicholas R, et al. Inflammatory intrathecal profiles and cortical damage in multiple sclerosis. *Ann Neurol*. 2018;83:739–755.
48. Bhargava P, Wicken C, Smith MD, et al. Trial of intrathecal rituximab in progressive multiple sclerosis patients with evidence of leptomeningeal contrast enhancement. *Mult Scler Relat Disord*. 2019;30:136–140.
49. Komori M, Lin YC, Cortese I, et al. Insufficient disease inhibition by intrathecal rituximab in progressive multiple sclerosis. *Ann Clin Transl Neurol*. 2016;3:166–179.
50. Neelapu SS, Tummala S, Kebriaei P, et al. Chimeric antigen receptor T-cell therapy - assessment and management of toxicities. *Nat Rev Clin Oncol*. 2018;15:47–62.
51. Bevan RJ, Evans R, Griffiths L, et al. Meningeal inflammation and cortical demyelination in acute multiple sclerosis. *Ann Neurol*. 2018;84:829–842.
52. Albert M, Antel J, Bruck W, Stadelmann C. Extensive cortical remyelination in patients with chronic multiple sclerosis. *Brain Pathol*. 2007;17:129–138.
53. Merkler D, Ernsting T, Kerschensteiner M, Brück W, Stadelmann C. A new focal EAE model of cortical demyelination: Multiple sclerosis-like lesions with rapid resolution of inflammation and extensive remyelination. *Brain*. 2006;129:1972–1983.
54. Calabrese M, Magliozzi R, Ciccarelli O, Geurts JJG, Reynolds R, Martin R. Exploring the origins of grey matter damage in multiple sclerosis. *Nat Rev Neurosci*. 2015;16:147–158.
55. Gardner C, Magliozzi R, Durrenberger PF, Howell OW, Rundle J, Reynolds R. Cortical grey matter demyelination can be induced by elevated pro-inflammatory cytokines in the subarachnoid space of MOG-immunized rats. *Brain*. 2013;136: 3596–3608.
56. Magliozzi R, Howell OW, Durrenberger P, et al. Meningeal inflammation changes the balance of TNF signalling in cortical grey matter in multiple sclerosis. *J Neuroinflamm*. 2019; 16:259.